Structure of Ni(II) and Ru(III) Ammine Complexes Grafted onto Mesoporous Silicate Sieve

Dominik Brühwiler and Heinz Frei*

Physical Biosciences Division, Mailstop Calvin Laboratory, Lawrence Berkeley National Laboratory, University of California, Berkeley, California 94720

Ru(III) and Ni(II) ammine complexes were grafted onto the pore surface of MCM-41 by ion exchange from basic aqueous solution. Covalent anchoring of the type M−O−Si (M = Ru or Ni) is obtained by this method. The structure of the grafted complexes was studied by UV−vis, FT-IR, and X-ray absorption spectroscopy. $[Ru(NH_3)_5Cl]^{2+}$ readily yielded monopodal grafting, while dehydration was needed in the case of $[Ru(NH_3)_6]^{3+}$ to achieve substitution of a NH_3 ligand with a siloxy group. The interaction of charge-compensating siloxy groups with remaining NH_3 ligands further stabilized the grafted Ru(III) centers. Dipodal grafting of Ni(II) was obtained with $[Ni(NH_3)_{6-x}(H_2O)_x]^{2+}$ ($x = 1$ or 2). Upon dehydration, the dipodally grafted Ni(II) complexes are converted in a reversible process to a tripodally anchored form through substitution of a H_2O ligand by a silanol group. The formation of layered Ni silicate structures, a dominant product in the Ni grafted amorphous silica, was not observed. This demonstrates that simple coordination complexes can be used for accomplishing covalent attachment of isolated metal centers on a mesoporous silicate sieve in high yield. Grafting of Ni(II) onto MCM-41 containing isolated Ti(IV) centers resulted in the formation Ti(IV)−O−Ni(II) moieties, which are of special interest for photochemical applications.

Introduction

Excited-state redox properties of transition metals that are either part of the framework or covalently anchored on the inner surface of micro- or mesoporous materials offer new opportunities for demanding photochemical transformations. Our approach is photochemistry at the gas−surface interface, and recent results on photoredox reactions of small molecules in Ti or V framework substituted silicate sieves by Anpo[1] and microporous Fe aluminophosphate or Ti silicalite from our laboratory[2] demonstrate the feasibility of the method. The discovery of mesoporous silicates (M41S family of materials, with MCM-41 as the most prominent member)[3] has opened up the preparation of transition-metal sieves by covalent anchoring of isolated metal centers on the pore surface via oxo-bridges. This method of introducing robust, site-isolated transition-metal chromophores and redox centers into the sieve considerably expands the variety of metals that can be used, because it removes limitations of isomorphous framework substitution, like the size of the metal atom, the selection of oxidation state, or the restriction to low concentration. Grafting of isolated transition-metal centers on mesoporous silicates through oxo-bridges has recently been reported for Ti,[4] Zr,[5] Cr,[6] Fe,[7] Mo,[8] V,[9] W,[10] and Rh,[11] as well as rare earth metals.[12] The majority of the materials have been prepared by ligand substitution reaction of an organometallic precursor with surface silanol groups.

Among the most interesting redox centers for photosynthetic transformations are Ru and Ni, but site-isolated grafting of these metals onto mesoporous silicates via oxo-bridges has so far not been described in the literature. In this paper, we report the covalent attachment of Ru(III) and Ni(II) centers onto MCM-41 using inorganic complexes rather than organometallic species as precursors. Inorganic species are employed because it obviates the need of calcination for removal of organic ligands, which is crucial if the selected metal oxidation state of the precursor

is to be preserved in the grafted material. Design of transition-metal sieves with well-defined oxidation states is important for photochemical applications and can be challenging for metals such as Ru and Ni, each featuring a whole series of accessible oxidation states. Previous studies using silica gel as support have shown that the adsorption of metal complexes by ion exchange at the silica−water interface leads to robust anchoring of the metal centers through formation of surface complexes with siloxy groups as ligands.[13] However, layered silicate structures were observed at the expense of isolated centers in the Ni grafting.[14] It will be shown in this paper that the ion exchange of Ni and Ru ammine complexes from basic aqueous solution results in covalent attachment of isolated metal centers in the pores of MCM-41 with minimal interference of cluster formation. Structural characterization of the anchored complexes was conducted by UV−vis, FT-IR, and X-ray absorption spectroscopy.

Experimental Section

Nomenclature. The following abbreviations are used: Ni−MCM41 for MCM-41 modified with Ni(II) ammine complexes, Ru−MCM41(N_6) for MCM-41 modified with $Ru(NH_3)_6^{3+}$, and Ru−MCM41(N_5Cl) for MCM-41 modified with $[Ru(NH_3)_5-Cl]^{2+}$. Samples with a specific Ni or Ru content are referred to as Ni−MCM41-*x*, Ru−MCM41(N_6)-*x*, or Ru−MCM41(N_5Cl)-*x*, where *x* denotes the amount of the corresponding metal in units of mmol per gram of MCM-41.

Synthesis of MCM-41. Two and two tenths grams of CTAB (cetyltrimethylammonium bromide, Aldrich) was dissolved under slight warming (30−40 °C) in a mixture of 52 mL of distilled H_2O and 24 mL of aqueous ammonia (28−30% NH_3, Aldrich). Ten milliliters of tetraethoxysilane (Fluka, puriss.) was slowly added under stirring to the clear solution and the resulting gel was further stirred for 3 h at room temperature. The mixture was then transferred to a Teflon lined autoclave and heated at 110 °C for 48 h. After cooling to room temperature, the product

---

was obtained by filtration, washed with 800 mL of distilled H_2O, and dried in air at room temperature. The template was removed by first heating at 300 °C for 2 h and subsequent calcination in air at 550 °C for 12 h. Heating rates were about 2 °C/min. This procedure is a modification of a previously reported method by Lin et al.[15]

Synthesis of Ni−MCM41. Ni−MCM41 was prepared following grafting methods for amorphous silica described by Bonneviot et al.[13e,16] The procedures were modified to prevent the dissolution of silica and to ensure the stability of the MCM-41 pore structure: 250 mg of calcined MCM-41 was dispersed in 10 mL of distilled H_2O containing 75 mg of $Ni(NO_3)_2 \cdot 6H_2O$ (Aldrich), 125 mg of NH_4NO_3 (Aldrich), and 4 mmol of NH_3. The suspension was shaken for 5 min, filtered, and washed with 10 mL of 0.45 M and 10 mL of 0.15 M aqueous ammonia. Exposure of the calcined MCM-41 to basic aqueous solution not only ensured facile loading of the Ni complex by ion exchange but also efficient rehydration of the silica pore surface as confirmed by intense H-bonded SiOH absorption in the IR spectrum (Figure 11). The product was dried in a vacuum at room temperature for 4 h. The amount of Ni adsorbed in the pores of MCM-41 was estimated by determining from the UV−vis spectra the residual amount of Ni(II) complexes in the exchange solution and in the washing solutions. Comparison of these values with the initial concentration of Ni(II) complexes in the exchange solution gave the Ni loading. The procedure described above typically yields samples with a Ni content of 0.7 mmol per gram of MCM-41, corresponding to a Si/Ni ratio of 24. Ni−MCM41 samples show a limited stability when stored under ambient conditions over several months. XRD revealed a decrease in long-range order of the MCM-41 accompanied by the development of a broad IR band at 3650 cm^{-1} suggesting the formation of nickel hydroxide or nickel silicate species.[14] The slow decomposition of the material is most likely associated with the liberation of NH_3 from the nickel coordination sphere through substitution by H_2O. For exposure of Ni−MCM41 to gaseous NH_3, anhydrous ammonia (Matheson) was used.

Synthesis of Ru−MCM41(N_6) and Ru−MCM41(N_5Cl). One hundred milligrams of calcined MCM-41 was dispersed in 10 mL of a 3 mM aqueous solution of $[Ru(NH_3)_6]Cl_3$ or $[Ru(NH_3)_5Cl]Cl_2$. Five 20 μL aliquots of a 0.5 M solution of NaOH were successively added under stirring over a period of 5 min. After filtration, the product was washed with 20 mL of distilled H_2O and 20 mL of methanol and subsequently dried in air at room temperature. The Ru loading was calculated as described for Ni−MCM41. Typically, 0.2 mmol of Ru(III) are adsorbed per gram of MCM-41 after the above treatment (Si/Ru = 83). Samples with lower loadings were prepared by reducing the amount of added NaOH. $[Ru(NH_3)_5Cl]Cl_2$ was synthesized from $[Ru(NH_3)_6]Cl_3$ (Aldrich) according to a procedure described by Vogt et al.[17]

Synthesis of Ti−MCM41 and NiTi−MCM41. Ti−MCM41 was prepared following a grafting method reported by Maschmeyer et al. using titanocene dichloride as a precursor.[4a] Ticp$_2$-Cl$_2$ (Aldrich, 97%), triethylamine (Fluka puriss., p.a.), and anhydrous chloroform (Aldrich, 99+ %) was used. The synthesis was performed under a dry nitrogen atmosphere. The bimetallic NiTi−MCM41 was prepared by applying the conditions for the synthesis of Ni−MCM41 to calcined Ti−MCM41.

Physical Measurements. UV−vis spectra were recorded with a Shimadzu UV-2100 spectrometer. For the measurement of self-supporting wafers of MCM-41 materials, the spectrometer was equipped with an integrating sphere (model ISR-260) and spectra were acquired in the diffuse reflectance mode. A pressed pellet of pure MCM-41 was used as reference. No absorption was detected in the 200−850 nm range for pure MCM-41 when measured against $BaSO_4$ powder. A specially designed stainless steel cell with a quartz window was used for measurements under vacuum.[18] Connecting the vacuum line to an IR transmission cell equipped with KCl windows holding an identical pellet allowed the simultaneous recording of FT-IR absorption spectra (Bruker model Vector33 spectrometer, 1 cm^{-1} resolution). Self-supporting wafers for UV−vis and FT-IR measurements were prepared by applying a pressure of 1 ton for 1 min to the powdered materials, resulting in pellets of about 15 mg and 12 mm diameter.

Powder X-ray diffraction (XRD) measurements were performed on a Siemens D-500 diffractometer with Cu Kα radiation (40 kV, 30 mA), a 2θ step size of 0.02°, and a 3-s counting time per step. Samples were dried for at least 3 h in a vacuum prior to the measurements.

Cl K-edge and Ru L$_{III}$-edge XANES spectra were recorded at beamline 9.3.1 of the Advanced Light Source at LBNL. Ring currents were in the 200−400 mA range (1.5 GeV). Measurements were conducted in transmission mode using a Si photodiode detector. The samples were prepared in the form of self-supporting wafers of about 20 mg and 12 mm diameter and evacuated at 2×10^{-7} Torr. Spectra were recorded with sampling intervals of 0.1 eV and 2-s counting time per data point.

Results

XRD Characterization of Grafted Materials. Prolonged exposure of MCM-41 to basic aqueous media usually leads to silicate hydrolysis resulting in a loss of long-range order.[19] To avoid structural degradation, the pH of the exchange solutions should not be higher than 10, and exchange times should be kept on the order of minutes. Fortunately, we found that the maximum loading at a given pH is achieved after just a few minutes, making longer exposure times unnecessary. Short exchange times also prevent the dissolution of silica into Si-$(OH)_4$ monomers, which lead to the formation of nickel silicates upon modification of silica gels with nickel ammine complexes.[14] Figure 1 shows the XRD patterns for samples obtained under the conditions described in the Experimental Section. Beck et al. observed that 3−5 peaks, which can be indexed on a hexagonal lattice ($hk0$ reflections only), are typical of MCM-41 materials.[3b] The patterns of Ni−MCM41 and Ru−MCM41 feature those distinct Bragg peaks, suggesting that the hexagonally ordered pore structure of MCM-41 is stable under the grafting conditions. From the position of the first diffraction peak (d_{100}), the repeat distance a_0 can be calculated ($a_0 = 2d_{100}/\sqrt{3}$).[3b] A value of $a_0 = 45$ Å is obtained for the samples shown in Figure 1. Assuming a pore wall thickness of 10 Å,[20,21] this results in a pore size of 35 Å.

$Ru(NH_3)_6^{3+}$ in MCM-41 (Ru−MCM41(N_6)). Figure 2, top, shows the diffuse reflectance spectrum (DRS) of as-synthesized Ru−MCM41(N_6) (trace a). It exhibits the same features as the spectrum of $[Ru(NH_3)_6]Cl_3$ in aqueous solution,[22] namely, a band with λ_{max} at 275 nm and a shoulder between 320 and 350 nm. While both of these bands contain a series of d−d transitions, the main absorption around 275 nm is generally attributed to a LMCT in the $Ru(NH_3)_6^{3+}$ complex.[23] The similarity of the DRS of Ru−MCM41(N_6) and the solution spectrum of $Ru(NH_3)_6^{3+}$ suggests that the ligand sphere of Ru(III) is unaltered upon exchange into MCM-41, indicating that the complex is adsorbed by electrostatic interaction with the negative surface charges generated by the deprotonation of silanol groups. The surface siloxy groups ($\equiv SiO^-$) can thus be regarded as counterions to the adsorbed $Ru(NH_3)_6^{3+}$ complexes.

Structure of Ni(II) and Ru(III) Ammine Complexes
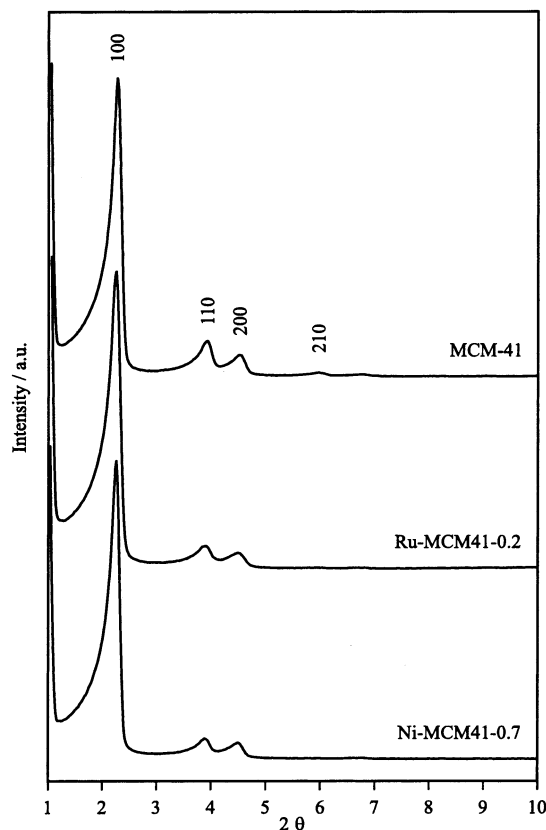
J. Phys. Chem. B, Vol. 107, No. 33, 2003 **8549**

Figure 1. XRD patterns of as-synthesized Ru−MCM41(N$_6$)−0.2 and Ni−MCM41−0.7. The pattern of the calcined MCM-41 used for the synthesis is shown for comparison.

This conclusion is further supported by the FT-IR spectrum (Figure 2, bottom, trace a) featuring an intense band at 1345 cm^{-1}, which is in good agreement with the value reported for the symmetric deformation of NH$_3$ in [Ru(NH$_3$)$_6$]Cl$_3$.[24] The corresponding asymmetric deformation mode around 1630 cm^{-1} is overlapped by the much more intense bending mode of adsorbed water molecules. The complexes could be efficiently recovered by washing with an aqueous solution of NaCl ($c <$ 1 M).

Evacuation of Ru−MCM41(N$_6$) leads to distinct changes of the absorption properties in the UV−vis and the IR (see Figure 2, traces b). Most remarkably, a broad band with a maximum at 402 nm develops, giving the material a deep yellow color. A very similar band has been reported for alkaline solutions of [Ru(NH$_3$)$_6$]Cl$_3$ and was assigned to a LMCT from a NH$_2^-$ ligand.[22] The presence of the strongly charge-donating amido group shifts the symmetric deformation of the remaining ammine ligands, which is known to be very sensitive toward changes of the effective charge on the metal center,[25] to lower energy. This shift manifests itself in the FT-IR difference spectrum by a decrease at 1345 cm^{-1} and the formation of a new band centered at 1300 cm^{-1} (see Figure 2). A more detailed record of the spectral changes upon evacuation is presented in Figure 3. We conclude that the following reaction takes place upon evacuation:

$$\equiv\text{SiO}^- + \text{Ru(NH}_3)_6{}^{3+} \rightarrow \equiv\text{SiOH} + [\text{Ru(NH}_3)_5\text{NH}_2]^{2+} \quad (1)$$
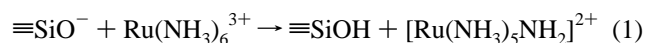
Reaction 1 is most likely initiated by the desorption of H$_2$O, indicated by a marked decrease at 1645 cm^{-1}, causing the removal of solvation spheres and facilitating close interaction between the adsorbed complexes and the siloxy groups.
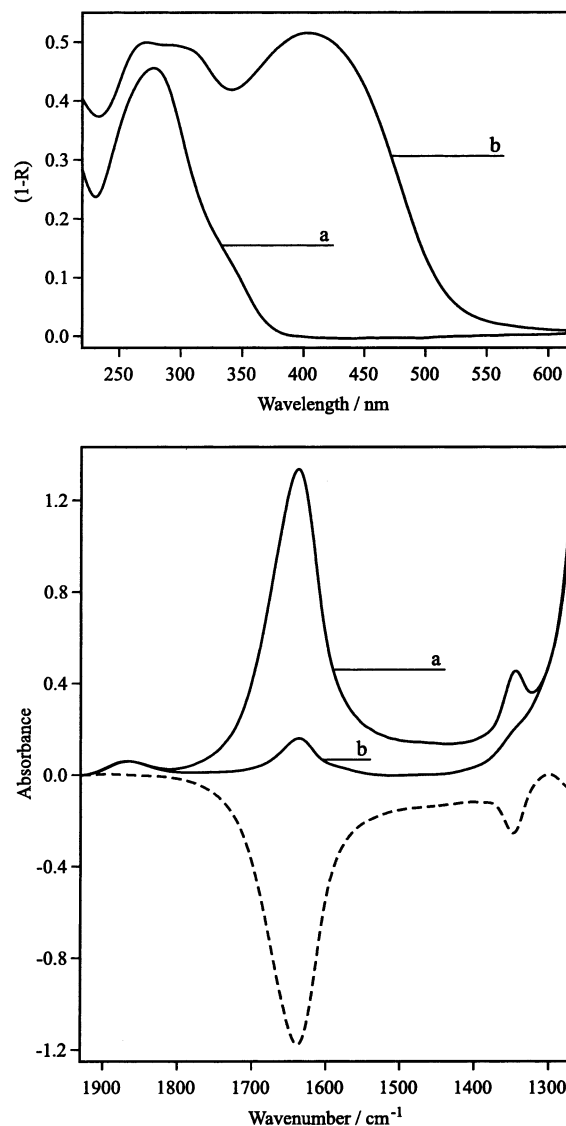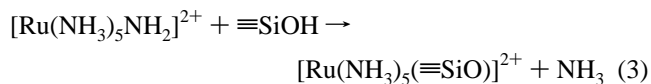

Figure 2. DRS (top) and FT-IR spectra (bottom) of as-synthesized Ru−MCM41(N$_6$)−0.2 under ambient conditions (traces a) and after evacuation to a pressure of 20 mTorr (traces b). The dashed line is the corresponding FT-IR difference spectrum. The weak absorption at 1870 cm^{-1} is a SiO combination band, while the edge at 1300 cm^{-1} is due to a band ascribed to SiO stretching vibrations.

The increasing absorption around 402 nm is accompanied by the development of a new band located around 300 nm (see Figure 3). The formation of this product band is caused by the limited stability of the deprotonated ruthenium hexaammine complex, which is known to undergo an aquation reaction in solution:[22,26]

$$[\text{Ru(NH}_3)_5\text{NH}_2]^{2+} + \text{H}_2\text{O} \rightarrow [\text{Ru(NH}_3)_5\text{OH}]^{2+} + \text{NH}_3 \quad (2)$$
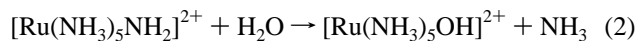
The absorption maximum of [Ru(NH$_3$)$_5$OH]$^{2+}$ is located at 295 nm and is due to a LMCT from the hydroxo ligand.[26,27] In MCM-41, we expect an analogous reaction involving a silanol group, thereby producing a monopodally grafted ruthenium ammine complex:

$$[\text{Ru(NH}_3)_5\text{NH}_2]^{2+} + \equiv\text{SiOH} \rightarrow$$
$$[\text{Ru(NH}_3)_5(\equiv\text{SiO})]^{2+} + \text{NH}_3 \quad (3)$$

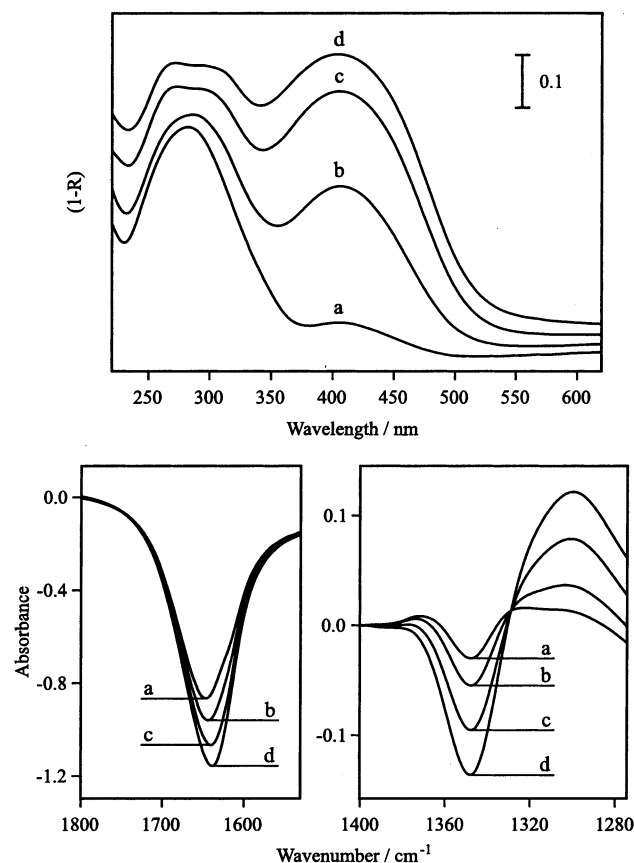In this case, we attribute the enhanced absorption around 300

Figure 3. DRS (top) and FT-IR difference spectra (bottom) of Ru−MCM41(N_6)−0.2 during evacuation: 1.5 Torr (traces a), 0.5 Torr (traces b), 0.1 Torr (traces c), and 0.02 Torr (traces d). The FT-IR difference spectra were calculated by ratioing against a spectrum taken before evacuation.
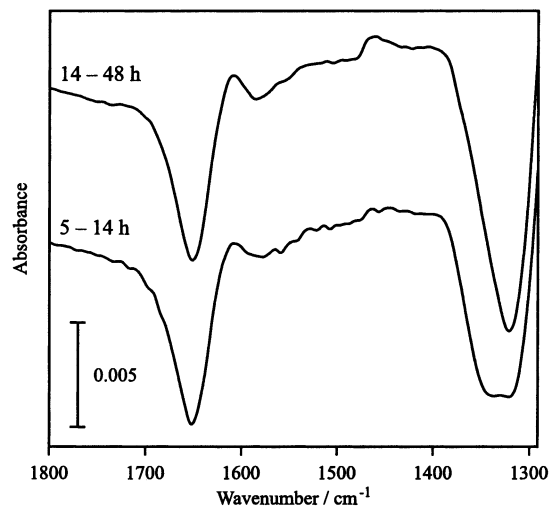

Figure 4. FT-IR difference spectra of Ru−MCM41(N_6)−0.2 at various times during prolonged evacuation at a pressure of 0.05 mTorr.
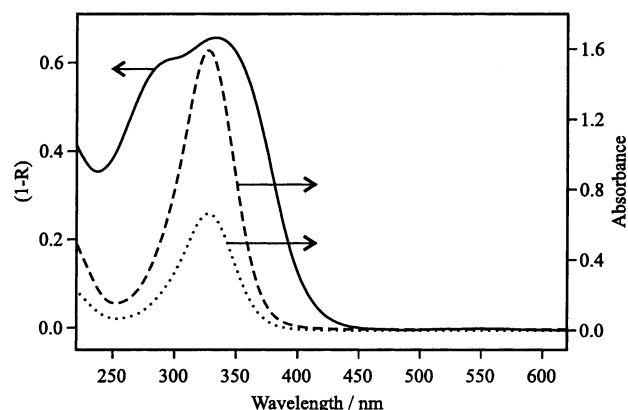

Figure 5. DRS of as-synthesized Ru−MCM41(N_5Cl)−0.2 (solid line) and absorption spectra of the exchange solution (1:3 diluted) before (dashed line) and after the exchange (dotted line).

nm to a LMCT from the siloxy group. The replacement of an amido group with a siloxy ligand according to reaction 3 would further result in a shift of $\delta_s(NH_3)$ to higher energy, yielding a band which lies between the respective bands for $Ru(NH_3)_6^{3+}$ (1345 cm^{-1}) and $[Ru(NH_3)_5NH_2]^{2+}$ (1300 cm^{-1}). Close examination of the corresponding FT-IR difference spectra in fact reveals a slight asymmetry in the product band, most probably caused by an additional absorption at approximately 1320 cm^{-1} (see Figure 3). No further loss at 1345 cm^{-1} is detected after approximately 24 h under high vacuum, indicating complete conversion of the hexaammine complex. Only minor changes occur upon prolonged evacuation: Most notably, the 402-nm band decreases, while a slight further increase is observed in the 300-nm region. After about 14 h under high vacuum, a loss at 1320 cm^{-1} dominates the FT-IR difference spectra (see Figure 4). This decrease at 1320 cm^{-1} is consistent with the loss of NH_3 ligands of ruthenium complexes containing one oxygen donor ligand. Hence, it suggests conversion of $[Ru(NH_3)_5(\equiv SiO)]^{2+}$ to dipodally grafted $[Ru(NH_3)_4(\equiv SiO)_2]^+$ species.

$[Ru(NH_3)_5Cl]^{2+}$ in MCM-41 (Ru−MCM41(N_5Cl)). Figure 5 shows the DRS of as-synthesized Ru−MCM41(N_5Cl) (solid curve). The spectra of the aqueous $[Ru(NH_3)_5Cl]Cl_2$ solution before and after the exchange is given for comparison. While the solution—even after the exchange—only contains $[Ru(NH_3)_5Cl]^{2+}$ (λ_{max} = 328 nm, assigned to Cl−Ru LMCT[28,29]), an enhanced absorption at shorter wavelength is observed in the DRS of Ru−MCM41(N_5Cl). This absorption is consistent with a LMCT from an oxygen donor ligand, indicating the presence of either $[Ru(NH_3)_5OH]^{2+}$ or $[Ru(NH_3)_5(\equiv SiO)]^{2+}$. The absorption in the O−Ru LMCT region was already found in wet Ru−

MCM41(N_5Cl) immediately after the exchange, and no significant spectral changes were observed in the DRS upon washing and drying. The fact that the exchange solution does not contain a band around 300 nm suggests that the corresponding species is not electrostatically adsorbed, as in $[Ru(NH_3)_6]^{3+}$ or $[Ru(NH_3)_5Cl]^{2+}$, but rather grafted onto the pore surface. The complex is therefore not involved in an ion exchange equilibrium which excludes $[Ru(NH_3)_5OH]^{2+}$ as a candidate, because we would expect this species to be present in the exchange solution as well. We conclude that the following ligand substitution takes place upon exchange of $[Ru(NH_3)_5Cl]^{2+}$ into MCM-41 under alkaline conditions:

$$[Ru(NH_3)_5Cl]^{2+} + \equiv SiO^- \rightarrow [Ru(NH_3)_5(\equiv SiO)]^{2+} + Cl^- \quad (4)$$
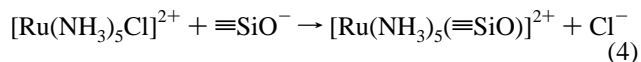
The FT-IR spectrum shows $\delta_s(NH_3)$ at 1325 cm^{-1}. Since we expect Cl$^-$ and $\equiv SiO^-$ to be weaker donors than NH_2^- but stronger donors than NH_3, the frequency of $\delta_s(NH_3)$ of $[Ru(NH_3)_5Cl]^{2+}$ and $[Ru(NH_3)_5(\equiv SiO)]^{2+}$ should lie between the respective values for $Ru(NH_3)_6^{3+}$ (1345 cm^{-1}) and $[Ru(NH_3)_5NH_2]^{2+}$ (1300 cm^{-1}). The absorption at 1325 cm^{-1} is therefore consistent with the presence of both $[Ru(NH_3)_5Cl]^{2+}$ and $[Ru(NH_3)_5(\equiv SiO)]^{2+}$. The electrostatically adsorbed $[Ru(NH_3)_5Cl]^{2+}$ complexes can be efficiently removed by repeated washing with an aqueous solution of NaCl, yielding MCM-41 containing grafted pentaammineruthenium(III) essentially free
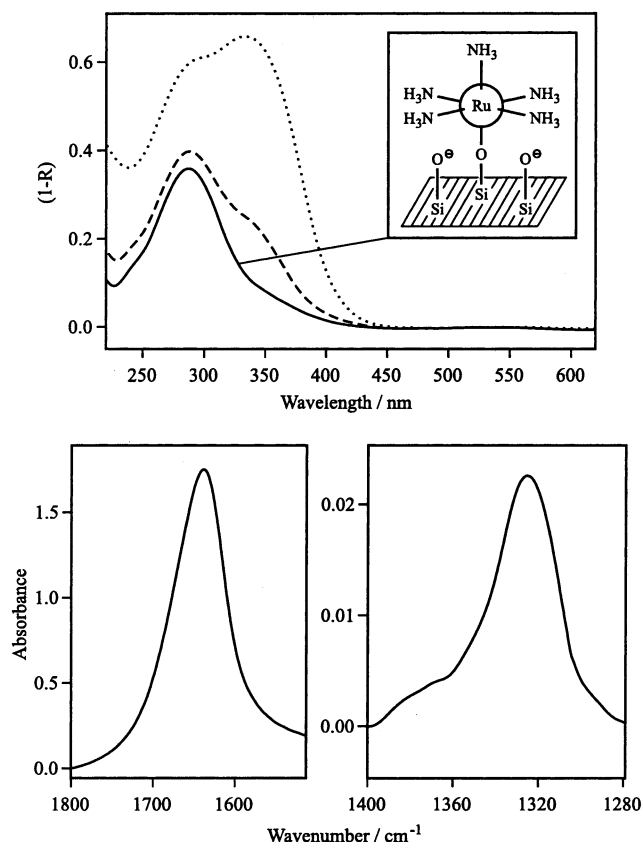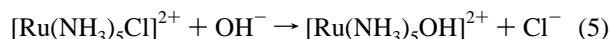
Structure of Ni(II) and Ru(III) Ammine Complexes

J. Phys. Chem. B, Vol. 107, No. 33, 2003 **8551**

Figure 6. DRS (top) and FT-IR spectra (bottom) of Ru−MCM41-(N_5Cl) after repeated washing with 20-mL portions of a 0.1 M aqueous solution of NaCl (10 min each): after three washing treatments (dashed line) and after five washing treatments (solid lines). The dotted line represents the spectrum of the as-synthesized material before the washing treatments. The FT-IR spectrum recorded after completion of the washing treatment was ratioed against pure MCM-41. The initial loading was 0.2 mmol of Ru per gram of MCM-41. Approximately 90% of the Ru complexes in the as-synthesized sample are present as electrostatically adsorbed $[Ru(NH_3)_5Cl]^{2+}$ and could be recovered by the washing treatment.
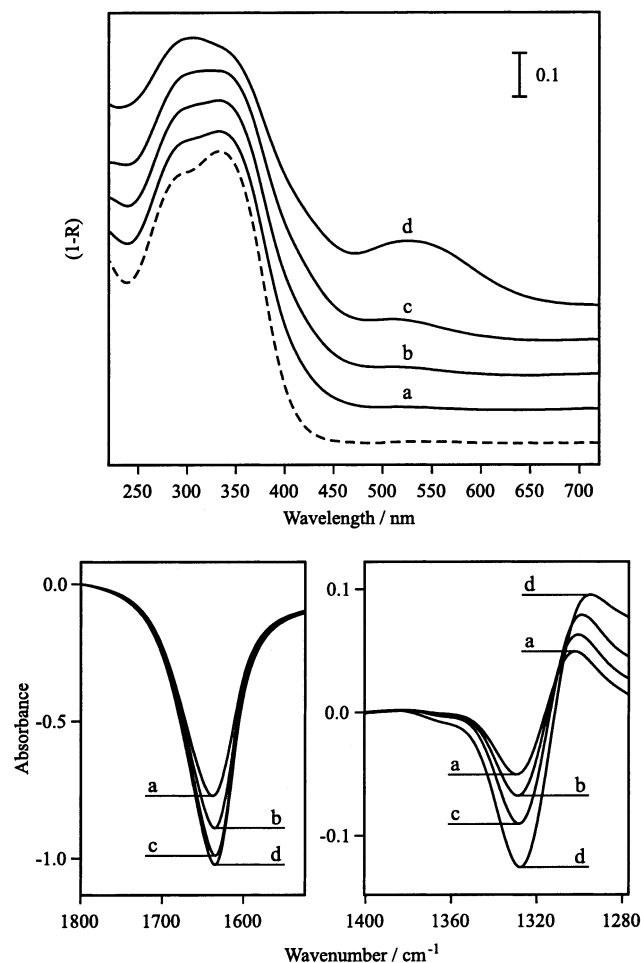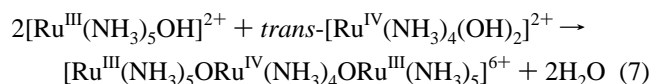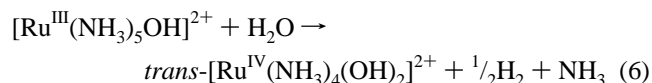

Figure 7. DRS (top) and FT-IR difference spectra (bottom) of Ru−MCM41(N_5Cl)−0.2 during evacuation: 0.5 Torr (traces a), 0.1 Torr (traces b), 0.02 Torr (traces c), and 0.1 mTorr (traces d). The dashed line indicates the DRS of the material under ambient conditions. The FT-IR difference spectra were calculated by ratioing against a spectrum taken before evacuation.

of $[Ru(NH_3)_5Cl]^{2+}$. The corresponding diffuse reflectance and FT-IR spectra are shown as solid traces in Figure 6.

Under the applied conditions, the formation of polynuclear Ru species typically involves ruthenium red.[30,31] This mixed-valence oxo-bridged ruthenium trimer can be identified by a strong absorption at 532 nm (ϵ_{max} = 21000, in water).[30] As can be seen in Figures 2 and 6, ruthenium red is not found in as-synthesized Ru−MCM41. However, when a sample of Ru−MCM41(N_5Cl) containing large amounts of electrostatically adsorbed $[Ru(NH_3)_5Cl]^{2+}$ was left in air for several days, a wine-red color began to develop. The formation of ruthenium red requires the presence of H_2O and sufficient mobility of the reactants. The first step leading to ruthenium red is proposed to be the hydrolysis of $[Ru(NH_3)_5Cl]^{2+}$:[32]

$$[Ru(NH_3)_5Cl]^{2+} + OH^- \rightarrow [Ru(NH_3)_5OH]^{2+} + Cl^- \quad (5)$$

Ruthenium red is then formed according to:[31]

$$[Ru^{III}(NH_3)_5OH]^{2+} + H_2O \rightarrow$$
$$trans\text{-}[Ru^{IV}(NH_3)_4(OH)_2]^{2+} + {}^1/_2H_2 + NH_3 \quad (6)$$

$$2[Ru^{III}(NH_3)_5OH]^{2+} + trans\text{-}[Ru^{IV}(NH_3)_4(OH)_2]^{2+} \rightarrow$$
$$[Ru^{III}(NH_3)_5ORu^{IV}(NH_3)_4ORu^{III}(NH_3)_5]^{6+} + 2H_2O \quad (7)$$

We found that the formation of ruthenium red is accelerated by treatment under vacuum. As in Ru−MCM41(N_6), evacuation of Ru−MCM41(N_5Cl) results in a shift of $\delta_s(NH_3)$ to lower energy, indicating the deprotonation of $[Ru(NH_3)_5Cl]^{2+}$ (see Figure 7). The chloride ligand in the resulting $[Ru(NH_3)_4NH_2$-Cl]^+$ complex is highly labile toward substitution.[32] This allows facile reaction with residual water molecules inside the pores of MCM-41, thereby producing $[Ru(NH_3)_5OH]^{2+}$ besides $[Ru(NH_3)_5(\equiv SiO)]^{2+}$. The increasing amount of species containing an oxygen donor ligand leads to an enhancement of the optical absorption around 300 nm and a concomitant decrease in the Cl−Ru LMCT region at 328 nm, clearly evident from the successive evacuation steps shown in Figure 7. The presence of residual water molecules and $[Ru(NH_3)_5OH]^{2+}$ complexes with sufficient mobility ultimately leads to the formation of ruthenium red, as observed by the band at 532 nm. The bottom part of Figure 7 shows that upon prolonged evacuation the δ_s-(NH_3) product band shifts further to lower frequencies. This effect is most likely a result of the strong overlap between the reactant and the product bands, yet it may also in part be due to the increasing concentration of ruthenium red, whose $\delta_s(NH_3)$ absorption is considerably redshifted (1276 cm^{-1}).[30] The formation of ruthenium red can be minimized by decreasing the Ru content or by exchanging the adsorbed $[Ru(NH_3)_5Cl]^{2+}$ complexes with suitable cations (e.g., Na$^+$).
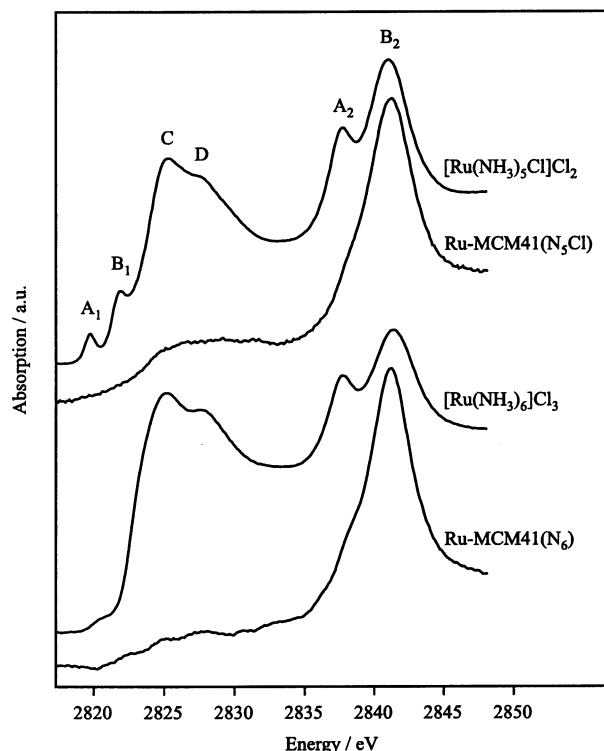
Figure 8. XANES spectra of Ru−MCM41(N_6)−0.03 and Ru−MCM41(N_5Cl)−0.03. The spectra of the corresponding precursor compounds [Ru(NH$_3$)$_6$]Cl$_3$ and [Ru(NH$_3$)$_5$Cl]Cl$_2$ (mechanical mixtures with MCM-41) are shown for comparison.

XANES spectra of Ru−MCM41(N_6) and Ru−MCM41-(N_5Cl). XANES spectra of Ru−MCM41(N_6)−0.03 and Ru−MCM41(N_5Cl)−0.03 along with the spectra of the corresponding precursor compounds are presented in Figure 8. Samples with low Ru content were chosen to minimize the formation of polynuclear complexes upon evacuation. Six peaks can be identified in the spectrum of [Ru(NH$_3$)$_5$Cl]Cl$_2$. Peaks A$_1$ and A$_2$ are assigned to transitions from the chlorine 1s level (A$_1$) and from the ruthenium 2p$_{3/2}$ core level (A$_2$) to the HOMO of the complex (t$_{2g}$, assuming octahedral symmetry). The HOMO contains a hole due to the d^5 low-spin configuration of Ru(III), therefore making transitions A$_1$ and A$_2$ possible. Peaks B$_1$ and B$_2$ are caused by transitions from the same core levels, the target orbital in this case being the LUMO (e$_g$).[33,34] Since [Ru(NH$_3$)$_6$]-Cl$_3$ does not contain a chloride ligand in its coordination sphere, transitions A$_1$ and B$_1$, which originate from the chlorine 1s level, cannot be observed in this complex. Peaks C and D in the Cl K-edge have been attributed by Sugiura et al.[33] to the continuum shape resonances of the outgoing electron trapped by the cage of the surrounding atoms. The XANES spectra of Ru−MCM41-(N_6) and Ru−MCM41(N_5Cl) are clearly different from the spectra of their respective precursor compounds; as a consequence of the ion exchange, the chloride ions acting as counterions in [Ru(NH$_3$)$_6$]Cl$_3$ and [Ru(NH$_3$)$_5$Cl]Cl$_2$ are replaced by siloxy groups, leading to a marked decrease in the Cl K-edge region. In Ru−MCM41(N_5Cl), there is still a significant absorption between 2820 and 2830 eV attributable to chloride introduced with [Ru(NH$_3$)$_5$Cl]$^{2+}$. The absence of preedge peaks similar to A$_1$ and B$_1$ confirms that the chloride present in Ru−MCM41(N_5Cl) is not part of the ligand sphere of Ru(III) as a consequence of the grafting of the complex to the pore surface. The Ru L$_{III}$-edge for Ru−MCM41(N_6) and Ru−MCM41(N_5-
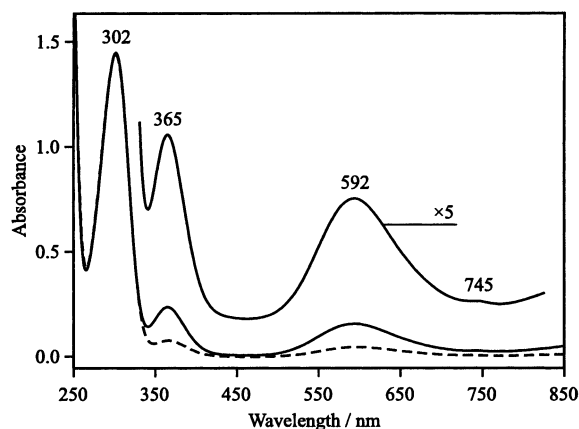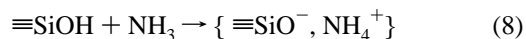

Figure 9. UV−vis spectra of the Ni(II) exchange solution before (solid line) and after (dashed line) the completion of the exchange.

TABLE 1: Electronic Transitions Observed in the Spectrum of the Ni(II) Exchange Solution

transition	λ/nm	assignment
λ_1	365	$^3T_{1g}(P) \leftarrow {}^3A_{2g}(F)$
λ_2	592	$^3T_{1g}(F) \leftarrow {}^3A_{2g}(F)$
λ_3	745	$^1E_g(D) \leftarrow {}^3A_{2g}(F)$

Cl) features only one peak (similar in energy to peak B$_2$ in the spectrum of the respective precursor compound). The quenching of peak A$_2$ upon adsorption of the complexes on MCM-41 and subsequent evacuation indicates an increase in electron density on Ru(III). The effective charge on the Ru centers in dehydrated Ru−MCM41 is apparently close to what would be expected from Ru(II). We attribute this effect to the strong interaction between NH$_3$ ligands and siloxy groups giving rise to hydrogen bonding and, in the extreme case, deprotonation. This result is consistent with the observation of amido groups in the corresponding UV−vis and FT-IR spectra. The strong-charge-donating characteristics of the amido group were also reported for the amido-bridged [(NH$_3$)$_4$Ru(NH$_2$)$_2$Ru(NH$_3$)$_4$]$^{4+}$ complex. Flood et al.[35] found that the Ru−NH$_3$ distances in this complex approach in value those observed for [Ru(NH$_3$)$_6$]-I$_2$.

Ni(II) Ammine Complexes in MCM-41 (Ni−MCM41). Unlike their Ru(III) analogues, Ni(II) ammine complexes feature no LMCT transitions at wavelengths longer than 250 nm. Analysis by UV−vis spectroscopy involves in this case d−d transitions only. Figure 9 shows the spectrum of the ammoniacal Ni(II) solution used for the exchange and compares it with the spectrum of the same solution after completion of the exchange. Assuming octahedral coordination of Ni(II), the observed absorption bands can be attributed to the electronic transitions compiled in Table 1. The absorption at 302 nm is due to a (π^* $\leftarrow$ n) transition of the uncomplexed nitrate ions.[36] Transition λ_1 is located at 395 nm for Ni(H$_2$O)$_6^{2+}$ and at 355 nm for Ni-(NH$_3$)$_6^{2+}$.[37] Using a linear approximation, it follows that substituting a NH$_3$ ligand with a H$_2$O ligand results in a bathochromic shift of 475 cm^{-1} for λ_1. With the maximum of λ_1 at 365 nm, the dominant species in the exchange solution is therefore not Ni(NH$_3$)$_6^{2+}$ but rather [Ni(NH$_3$)$_5$H$_2$O]$^{2+}$ and [Ni-(NH$_3$)$_4$(H$_2$O)$_2$]$^{2+}$. After completion of the exchange and filtration, the concentration of Ni(II) complexes in the solution has clearly decreased, while the absorption band at 302 nm remains unchanged (see Figure 9). This is consistent with the following ion exchange:
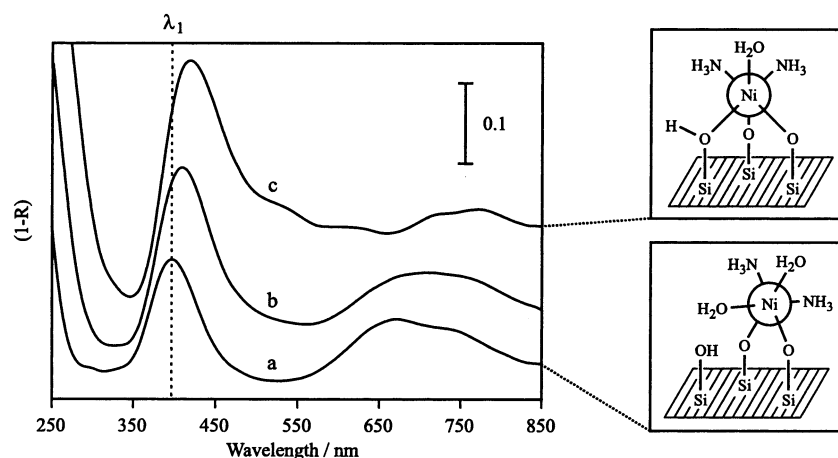
$$\equiv\text{SiOH} + \text{NH}_3 \rightarrow \{\equiv\text{SiO}^-, \text{NH}_4^+\} \qquad (8)$$

Structure of Ni(II) and Ru(III) Ammine Complexes

J. Phys. Chem. B, Vol. 107, No. 33, 2003 **8553**

Figure 10. DRS of Ni−MCM41−0.7: As-synthesized (trace a), after evacuation to 80 mTorr (trace b), and to 0.04 mTorr (trace c). A possible configuration of the isolated Ni centers in the hydrated and the dehydrated state of Ni−MCM41 is shown schematically on the right.

TABLE 2: Calculated Energy of λ_1 for Different Configurations of the Adsorbed Ni(II) Complexes in Hydrated Ni-MCM41

| | number of ligands | | | |
configuration	NH_3	H_2O	$\equiv SiO^-$	
I	2	2	2	390
II	1	4	1	392
III	2	1	3	394
IV	0	6	0	395
V	1	3	2	397
VI	2	0	4	399
VII	0	5	1	400

and

$$2\{\equiv SiO^-, NH_4{}^+\} + [NiL_6]^{2+} \rightarrow$$
$$\{2(\equiv SiO^-), [NiL_6]^{2+}\} + 2NH_4{}^+ \quad (9)$$
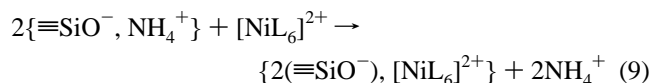
whereby L = NH_3 or H_2O.

The question arises whether the siloxy groups enter the ligand sphere of nickel by substituting NH_3 or H_2O ligands, that is, whether grafting occurs. Figure 10, trace a, shows the DRS of as-synthesized Ni−MCM41−0.7 (after washing, drying, and rehydration under ambient conditions). In agreement with the spectra of the exchange solution (see Figure 9), no absorption characteristic of nitrate ions (λ_{max} = 302 nm) is detected. Transition λ_1 is now found at 395 nm. A similar bathochromic shift of λ_2 causes mixing with the spin-forbidden transition λ_3, which is less sensitive to changes of the ligand field strength, hence generating a feature consisting of two overlapping bands of similar intensity at approximately 670 and 750 nm. Comparison of the energy of λ_1 for complexes in the exchange solution (365 nm) and for complexes in as-synthesized Ni−MCM41 (395 nm) reveals a bathochromic shift of 2080 cm^{-1}. This shift is either caused by the substitution of NH_3 with H_2O ($\Delta\lambda_1$ = −475 cm^{-1}) or by the substitution of H_2O with siloxy groups ($\Delta\lambda_1$ = −300 cm^{-1}).[13e] Using the relative shifts induced by these ligand substitutions, one can find the configurations consistent with the observed energy of λ_1. Table 2 lists configurations with $\lambda_1 \approx$ 395 nm. Configurations III and VI are unlikely for hydrated samples, since they would lead to a strained geometry. The presence of NH_3 can be probed by FT-IR spectroscopy. As shown in Figure 11, trace b, the FT-IR spectrum of Ni−MCM41−0.7 shows significant bands attributable to vibrations of adsorbed NH_3.[38] In the NH_3 stretching region, absorptions were found at 3385, 3290, 3220 (weak), and 3195 cm^{-1}. In the bending region, the band at 1621 cm^{-1}
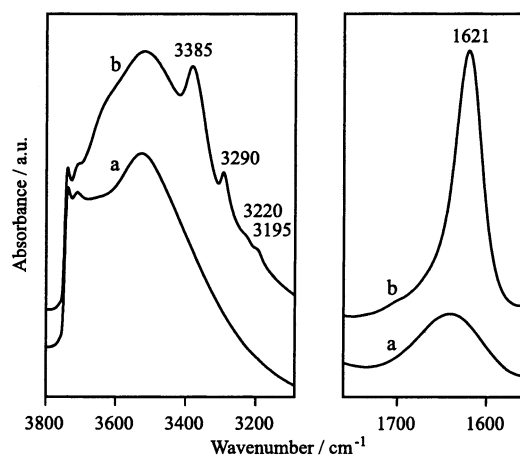

Figure 11. FT-IR spectra of MCM-41 (after treatment under the conditions used for Ni(II) exchange, but without the nickel source; trace a) and Ni−MCM41−0.7 (trace b). The absorption at 3737 cm^{-1} is due to stretching vibrations of free silanol groups, while the band at 3710 cm^{-1} most likely corresponds to a stretching vibration of a silanol group in which the O atom forms a hydrogen bond with the H atom of an adjacent silanol group. The very broad band centered at approximately 3520 cm^{-1} is due to stretching vibrations of chains of hydrogen-bonded silanol groups (silanol nests). The spectra were recorded after overnight evacuation to a pressure of 0.04 mTorr.

is assigned to $\delta_{as}(NH_3)$.[39] The shoulder in the high-frequency part of this band is due to residual water molecules and to a weak SiO overtone at 1640 cm^{-1}.[40] Contrary to the Ru(III) ammine complexes, the presumably much stronger $\delta_s(NH_3)$ cannot be observed. Situated at 1176 cm^{-1} (as found for [^{58}Ni-(NH$_3$)$_6$]Cl$_2$),[39] it is obscured by the totally absorbing SiO stretching vibrations. To confirm that the detected NH_3 is indeed associated with Ni(II), a sample of calcined MCM-41 was treated under the same conditions as used for the synthesis of Ni−MCM41−0.7 but without dissolved Ni(NO$_3$)$_2$·6H$_2$O. As shown in Figure 11, trace a, the FT-IR spectrum of MCM-41 treated according to this procedure does not feature the bands mentioned above. We therefore conclude that they are due to NH_3 coordinated to Ni(II). The absorptions at 3385 and 3290 cm^{-1} can be assigned to the asymmetric and the symmetric stretching mode, respectively, of NH_3 coordinated to Ni(II), while the weaker absorptions at 3220 and 3195 cm^{-1} have been ascribed in the literature to the corresponding vibrations of $NH_4{}^+$ or possibly $NH_2{}^-$.[38,41,42] Since we did not observe the respective bending vibrations (approximately 1530 cm^{-1} for $NH_2{}^-$ and 1430 cm^{-1} for $NH_4{}^+$),[30,38,41,42] the assignment of the bands at

8554 *J. Phys. Chem. B, Vol. 107, No. 33, 2003*

Brühwiler and Frei

3220 and 3195 cm^{-1} is not entirely clear. Nevertheless, these results strongly favor configurations containing NH$_3$ ligands, namely, I, II, and V (see Table 2). On the basis of previous studies concerning the adsorption of Ni(II) ammine complexes on silica gel and the low stability of the H$_2$O ligands against substitution, the monopodally grafted configuration II seems unlikely.[13e] We therefore assume that Ni(II) is coordinated to two siloxy groups and to one or two NH$_3$ ligands in as-synthesized, hydrated Ni−MCM41. The remaining ligands in the 6-fold coordination are H$_2$O.

Evacuation of Ni−MCM41 shifts λ_1 to 420 nm accompanied by an increase in the intensity of the band (see Figure 10, traces b and c). A further bathochromic shift is also observed for λ_2, although mixing between λ_2 and λ_3 complicates the spectral analysis in this region. Additionally, weak absorptions at 540 and 620 nm develop after prolonged treatment under high vacuum. These vacuum-induced changes are reversible upon rehydration of the samples. The bathochromic shift of transition λ_1 upon evacuation indicates a further decrease in the ligand field strength experienced by Ni(II). Assuming that nickel retains a 6-fold coordination under the applied conditions, this suggests the replacement of H$_2$O or NH$_3$ with weaker field ligands. Unfortunately, the relative shifts of λ_1 induced upon ligand substitution (−475 cm^{-1} for H$_2$O replacing NH$_3$ and −300 cm^{-1} for ≡SiO$^-$ replacing H$_2$O)[13e] are not valid for samples after evacuation. We found that under these conditions, the energy of transition λ_1 is too low to be explained on the basis of the $\Delta\lambda_1$ values mentioned above. The NH$_3$ ligands show considerable stability against substitution. Monitoring of the NH$_3$ stretching absorption upon evacuation of Ni−MCM41−0.7 under high vacuum (16 h), subsequent exposure to 10 Torr of H$_2$O (30 min), and dehydration under high vacuum (16 h) revealed a total loss of NH$_3$ ligand absorption of only 5−10%. Substitution of NH$_3$ ligands upon evacuation is therefore ruled out. Given the relative lability of Ni(II)-coordinated H$_2$O ligands toward substitution, the redshift of λ_1 during evacuation strongly suggests the substitution of H$_2$O ligands by siloxy or silanol groups. The introduction of additional surface groups into the ligand sphere of Ni(II) leads to an increasing deviation from a centrosymmetrical environment, indicated by the enhanced intensity of λ_1 and the detection of new absorptions in the UV−vis.[43] For silica gel, the coordination of Ni(II) to two siloxy groups has been reported to yield a stable structure showing little deviation from octahedral symmetry.[13c,13e] Similarly, coordination to two siloxy groups already occurs in hydrated Ni−MCM41 samples. This indicates that the structure generated upon evacuation corresponds to the coordination of Ni(II) to more than two, most likely three, surface groups. Because of the principle of charge neutrality, the number of siloxy groups per Ni(II) center is limited to two. It is therefore very likely that the third surface group replacing a H$_2$O ligand upon evacuation is in fact a silanol.

To estimate the number of NH$_3$ ligands in the grafted Ni(II) complex, a sample of Ni−MCM41−0.7 was evacuated overnight and exposed to 500 Torr of NH$_3$ gas for a period of 5 h. After renewed evacuation overnight, the IR spectrum of the sample was compared to the corresponding spectrum before NH$_3$ exposure. As can be seen in Figure 12, top, the amount of NH$_3$ coordinated to nickel increased by a factor of 1.7 following the above treatment. No significant increase of the NH$_3$ content was found after repeated exposure of Ni−MCM41 to NH$_3$ followed by evacuation, indicating complete substitution of H$_2$O ligands. Contrary to Ni−MCM41, exposure of plain MCM-41 to 500 Torr of NH$_3$ followed by evacuation did not produce any
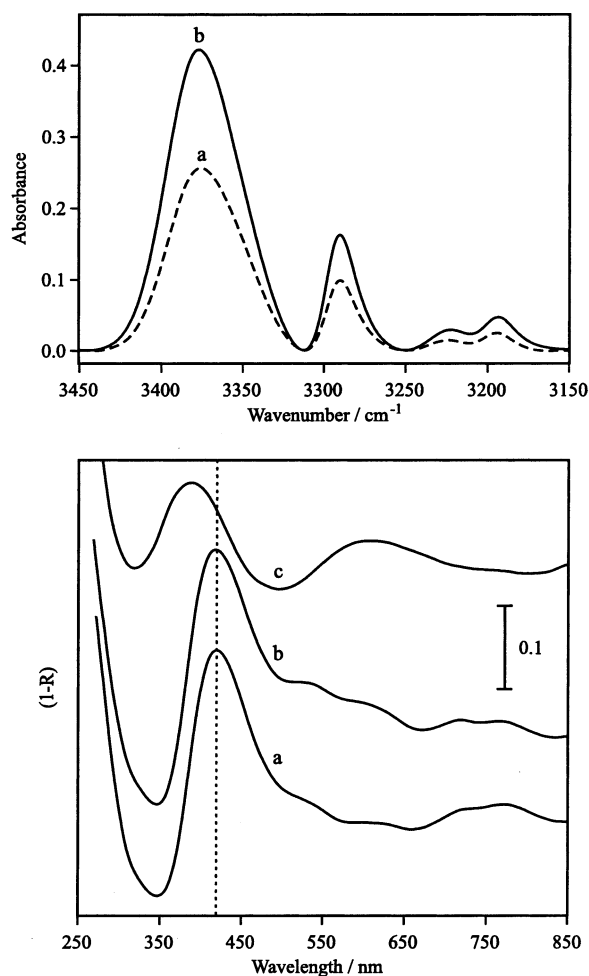

Figure 12. FT-IR spectra (top) and DRS (bottom) of Ni−MCM41−0.7 after evacuation to 0.04 mTorr (traces a). Traces b are spectra of the same sample after exposure to NH$_3$ (500 Torr, 5 h) and subsequent evacuation to 0.04 mTorr. Also shown is the DRS taken after 1 min of NH$_3$ exposure (500 Torr, trace c). The FT-IR spectra were corrected for the sloping baseline caused by the absorption of hydrogen-bonded silanol groups.

significant spectral changes in the IR or UV−vis. Given the similarity of the DRS before and after NH$_3$ exposure (see Figure 12, bottom, traces a and b), coordination to three surface groups can still be assumed after the NH$_3$ treatment. Since all H$_2$O ligands have been replaced, this indicates that now three NH$_3$ ligands complete the 6-fold coordination of Ni(II). The 1.7-fold increase of NH$_3$ content leading to this configuration suggests initial configurations with one or two NH$_3$ ligands, which is in agreement with our previous conclusions based on the position of λ_1 in the DRS of hydrated Ni−MCM41 (see Table 2, configurations I and V).

Exposure of dehydrated Ni−MCM41 to NH$_3$ has a remarkable effect on the DRS. Adsorption of NH$_3$ immediately leads to a hypsochromic shift of λ_1 and a concomitant intensity decrease (see Figure 12, trace c). Rehydration has a very similar effect, although the hypsochromic band shifts are in this case smaller. We attribute this effect to the breaking of a strained Si−O(H)−Ni bond through substitution of the surface group by NH$_3$ or H$_2$O, respectively, therefore reestablishing a higher symmetry around the nickel centers.

NiTi−MCM41. It has been established that calcined Ti−MCM41 grafted by the Ticp$_2$Cl$_2$ method contains high concentrations of tripodally anchored ≡TiOH groups.[4a,44] Application of the Ni(II) grafting method to Ti−MCM41 is therefore

Structure of Ni(II) and Ru(III) Ammine Complexes

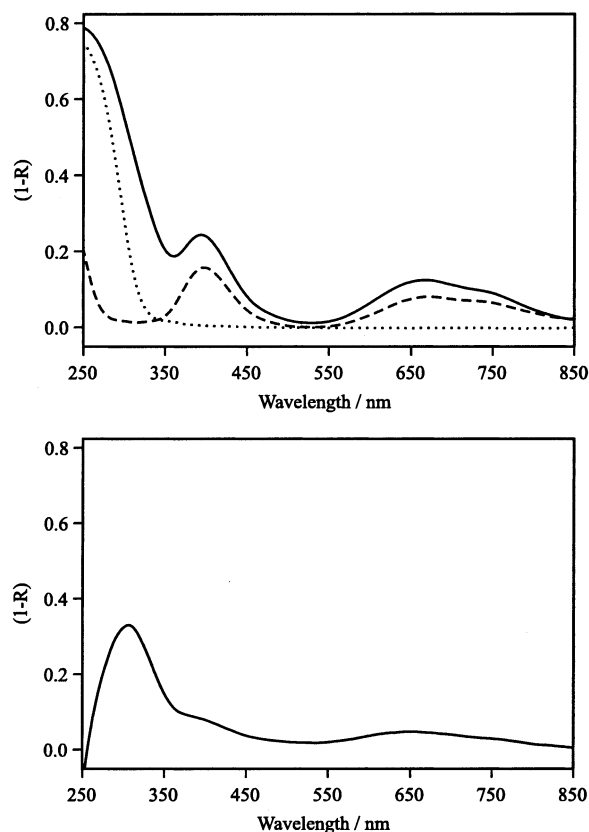*J. Phys. Chem. B, Vol. 107, No. 33, 2003* **8555**

Figure 13. DRS of as-synthesized NiTi−MCM41 (top, solid line) containing 0.7 mmol Ni and 0.2 mmol Ti (per gram of MCM-41). Monometallic samples of the same metal loading are shown for comparison: Ni−MCM41 (dashed line) and Ti−MCM41 (dotted line). The difference spectrum between NiTi−MCM41 and the two monometallic systems is shown in the bottom panel.

expected to yield a substantial amount of dipodally grafted nickel centers containing a ≡TiO⁻ group in their ligand sphere. We found the grafted Ti(IV) centers to be stable under the nickel grafting conditions. Exposure of Ti−MCM41 to an ammoniacal solution of NH_4NO_3 (same concentrations as used for the grafting of Ni) did not produce any changes in the optical absorption spectrum of the material, therefore establishing that the formation of TiO_2 clusters does not occur. As shown in Figure 13, the optical absorption spectrum of NiTi−MCM41 is not reproduced by a superposition of the spectra of the respective monometallic systems. The additional absorptions in NiTi−MCM41 can thus be attributed to the interaction of Ti(IV) and Ni(II) through Ni−O−Ti bridges. Figure 13, bottom, presents the difference spectrum calculated from the spectra of the bimetallic (NiTi−MCM41) and the two monometallic systems (Ni−MCM41 and Ti−MCM41) shown in the top panel of the same figure. If features a strong absorption around 300 nm with a tail extending into the visible region. The latter is overlapped by weak shoulders around 400, 650, and 750 nm indicative of increased intensity of Ni(d−d) transitions. The only assignment we can conceive of for the UV absorption and its adjoining visible tail is a metal-to-metal charge transfer (MMCT) from Ni(II) to Ti(IV).[45] The concurrent enhancement of the Ni-(d−d) bands confirms that the symmetry of the Ni(II) environment is further decreased, presumably because of the presence of ≡TiO⁻ in the Ni(II) ligand sphere.

Discussion and Conclusions

The combined use of UV−vis, FT-IR, and X-ray absorption spectroscopies furnishes a detailed insight into the grafting process and the structure of Ru(III) and Ni(II) ammine complexes covalently anchored on the pore surface of MCM-41 sieve. For Ni(II) with the sieve in the hydrated state, we find the same dipodal anchoring proposed for Ni(II) ammine complexes grafted onto amorphous silica (Aerosil 380, PBM 500, Spherosil XOA 400).[13c,e] In MCM-41, however, UV−vis and infrared evidence suggests that dehydration results in further stabilization of the Ni(II) complex by formation of a third Ni−O(H)−Si pod. Having a strained geometry, this complex is readily converted back to its dipodal form upon rehydration. By contrast, the Ru(III) ammine complex undergoes only monopodal grafting (except after prolonged evacuation) reflecting the higher strength of the Ru−NH_3 interaction compared to Ni−NH_3. However, the intensity changes of the Ru L_{III}-edge absorption bands and the infrared frequency shifts of the NH_3 bending modes signal additional stabilization of the anchored Ru(III) complex by interaction of surface siloxy groups with the remaining NH_3 ligands.

A remarkable difference between grafting of Ni(II) ammine complexes on MCM-41 and amorphous silica is the absence of Ni silicate formation in the case of the mesoporous sieve. While dehydration of Ni−MCM41 results in further stabilization of the isolated Ni centers by an additional link to a silanol group, Ni(II) ammine grafted on amorphous silica led to the formation of Ni silicates (phyllosilicates) irrespective of Ni loading or the pH of the exchange solution.[14a,16,46] Aside from a Ni−O−Ni signature in the EXAFS spectrum, these layered Ni silicates have characteristic infrared absorptions at 670 and 710 cm⁻¹,[14a] neither of which was detected in Ni−MCM41 before or after dehydration. Moreover, the reproducibility of the UV−vis and infrared spectra of the grafted Ni(II) ammine species corroborates that no agglomeration occurs under repeated washing, drying, and rehydration. An obvious factor that may help suppress the formation of undesired Ni silicates in MCM-41 is the short exposure time to basic solution (pH = 10); a period of 5 min was sufficient for the completion of ion exchange and grafting, while the same process took 24 h in the case of amorphous silica.[14a] At this high pH, dissolution of silica—a process that facilitates the formation of phyllosilicates—becomes significant.[19] The high pH treatment of the calcined MCM-41 during the grafting process ensures that the sieve is rehydrated, resulting in a density of SiOH groups that is within a factor of 2 the same as that of amorphous silica (2.5−3 nm⁻² versus 5−8 nm⁻²).[47] Another factor that disfavors agglomeration of Ni centers is the compartmentalization of the inner silica surface by the unidimensional channel system of MCM-41, which severely restricts the mobility of the complexes. Opportunities for Ni clustering are expected to be far greater on the open surface of amorphous silica. Furthermore, it is conceivable that differences in the energetics of covalent attachment of Ni(II) centers versus condensation in the form of Ni silicates favors single-site grafting in the mesoporous sieve.

Independent of the detailed factors responsible for the grafting result, the high selectivity in terms of isolated Ni(II) centers in MCM-41 demonstrates that simple coordination complexes can be used to covalently attach metal centers on a mesoporous silicate sieve in a pre-selected oxidation state. This is of crucial importance for photochemical applications since the redox reactivity of the excited state of the anchored metal depends on its oxidation state. Grafting methods that required calcination procedures, as in organometallic precursors, cannot be employed because the oxidation state of the precursor is not preserved. This holds especially for reducing states of metals that feature an entire series of accessible oxidation states.

The observation of the MMCT absorption, which indicates the formation of a surface-anchored Ti(IV)−O−Ni(II) moiety, points to opportunities for photoactivation of Ti centers by visible light. The nature of the optical absorption shown in Figure 13 is

$$\text{Ti(IV)}-\text{O}-\text{Ni(II)} \rightarrow \text{Ti(III)}-\text{O}-\text{Ni(III)} \qquad (10)$$
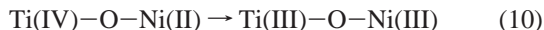
resulting in a transiently reduced Ti(III) center. The latter is the reducing site of demanding photosynthetic reactions in framework Ti silicate sieves.[1,2] However, UV photons are required because Ti(III) is generated by a LMCT from framework oxygen to Ti(IV), which absorbs only at wavelengths shorter than 300 nm. Metal-to-metal charge-transfer chromophores such as Ti(IV)−O−Ni(II) allow us to engage a second metal as electron donor rather than framework oxygen. This opens up a way of reducing the Ti centers by longer wavelength, visible light.

References and Notes

(1) (a) Anpo, M.; Zhang, S. G.; Yamashita, H. In *Stud. Surf. Sci. Catal.*; Hightower, J. W., Delgass, W. N., Iglesia, E., Bell, A. T., Eds.; Elsevier: Amsterdam, 1996; Vol. 101, p 941. (b) Zhang, S. G.; Ichihashi, Y.; Yamashita, H.; Tatsumi, T.; Anpo, M. *Chem. Lett.* **1996**, 895. (c) Zhang, S. G.; Fujii, Y.; Yamashita, H.; Koyano, K.; Tatsumi, T.; Anpo, M. *Chem. Lett.* **1997**, 659. (d) Anpo, M.; Yamashita, H.; Ikeue, K.; Fujii, Y.; Zhang, S. G.; Ichihashi, Y.; Park, D. R.; Suzuki, Y.; Koyano, K.; Tatsumi, T. *Catal. Today* **1998**, *44*, 327.

(2) (a) Ulagappan, N.; Frei, H. *J. Phys. Chem. A* **2000**, *104*, 490. (b) Yeom, Y. H.; Frei, H. *J. Phys. Chem. A* **2002**, *106*, 3350. (c) Ulagappan, N.; Frei, H. *J. Phys. Chem. A* **2000**, *104*, 7834. (d) Yeom, Y. H.; Frei, H. *J. Phys. Chem. A* **2001**, *105*, 5534. (e) Lin, W.; Frei, H. *J. Am. Chem. Soc.* **2002**, *124*, 9292.

(3) (a) Kresge, C. T.; Leonowicz, M. E.; Roth, W. J.; Vartuli, J. C.; Beck, J. S. *Nature* **1992**, *359*, 710. (b) Beck, J. S.; Vartuli, J. C.; Roth, W. J.; Leonowicz, M. E.; Kresge, C. T.; Schmitt, K. D.; Chu, C. T. W.; Olson, D. H.; Sheppard, E. W.; McCullen, S. B.; Higgins, J. B.; Schlenker, J. L. *J. Am. Chem. Soc.* **1992**, *114*, 10834.

(4) (a) Maschmeyer, T.; Rey, F.; Sankar, G.; Thomas, J. M. *Nature* **1995**, *378*, 159. (b) Wu, P.; Iwamoto, M. *J. Chem. Soc., Faraday Trans.* **1998**, *94*, 2871.

(5) (a) Morey, M. S.; Stucky, G. D.; Schwarz, S.; Fröba, M. *J. Phys. Chem. B* **1999**, *103*, 2037. (b) Zhang, W. H.; Shi, J. L.; Wang, L. Z.; Yan, D. S. *Mater. Lett.* **2000**, *46*, 35.

(6) Rao, R. R.; Weckhuysen, B. M.; Schoonheydt, R. A. *Chem. Commun.* **1999**, 445.

(7) (a) Nozaki, C.; Lugmair, C. G.; Bell, A. T.; Tilley, T. D. *J. Am. Chem. Soc.* **2002**, *124*, 13194. (b) Stockenhuber, M.; Hudson, M. J.; Joyner, R. W. *J. Phys. Chem. B* **2000**, *104*, 3370.

(8) Shannon, I. J.; Maschmeyer, T.; Oldroyd, R. D.; Sankar, G.; Thomas, J. M.; Pernot, H.; Balikdjian, J. P.; Che, M. *J. Chem. Soc., Faraday Trans.* **1998**, *94*, 1495.

(9) (a) Luan, Z.; Kevan, L. *J. Phys. Chem. B* **1997**, *101*, 2020. (b) Zhu, K.; Ma, Z.; Zou, Y.; Zhou, W.; Chen, T.; He, H. *Chem. Commun.* **2001**, 2552. (c) Morey, M.; Davidson, A.; Eckert, H.; Stucky, G. *Chem.*

Mater. **1996**, *8*, 486. (d) Van Der Voort, P.; Morey, M.; Stucky, G. D.; Mathieu, M.; Vansant, E. F. *J. Phys. Chem. B* **1998**, *102*, 585. (e) Oldroyd, R. D.; Sankar, G.; Thomas, J. M.; Hunnius, M.; Maier, W. F. *J. Chem. Soc., Faraday Trans.* **1998**, *94*, 3177.

(10) Morey, M. S.; Bryan, J. D.; Schwarz, S.; Stucky, G. D. *Chem. Mater.* **2000**, *12*, 3435.

(11) Pillinger, M.; Nunes, C. D.; Vaz, P. D.; Valente, A. A.; Gonçalves, I. S.; Ribeiro-Claro, P. J. A.; Rocha, J.; Carlos, L. D.; Kühn, F. E. *Phys. Chem. Chem. Phys.* **2002**, *4*, 3098.

(12) Anwander, R.; Görlitzer, H. W.; Gerstberger, G.; Palm, C.; Runte, O.; Spiegler, M. *J. Chem. Soc., Dalton Trans.* **1999**, 3611.

(13) (a) Burwell, R. L.; Pearson, R. G.; Haller, G. L.; Tjok, P. B.; Chock, S. P. *Inorg. Chem.* **1965**, *4*, 1123. (b) Schindler, P. W.; Fürst, B.; Dick, R.; Wolf, P. U. *J. Coll. Interface Sci.* **1976**, *55*, 469. (c) Hathaway, B. J.; Lewis, C. E. *J. Chem. Soc. A* **1969**, 1176. (d) Anderson, J. H. *J. Catal.* **1972**, *26*, 277. (e) Bonneviot, L.; Legendre, O.; Kermarec, M.; Olivier, D.; Che, M. *J. Colloid Interface Sci.* **1990**, *134*, 534.

(14) (a) Clause, O.; Kermarec, M.; Bonneviot, L.; Villain, F.; Che, M. *J. Am. Chem. Soc.* **1992**, *114*, 4709. (b) Kermarec, M.; Carriat, J. Y.; Burattin, P.; Che, M.; Decarreau, A. *J. Phys. Chem.* **1994**, *98*, 12008.

(15) Lin, W.; Cai, Q.; Pang, W.; Yue, Y.; Zou, B. *Microporous Mesoporous Mater.* **1999**, *33*, 187.

(16) Bonneviot, L.; Clause, O.; Che, M.; Manceau, A.; Dexpert, H. *Catal. Today* **1989**, *6*, 39.

(17) Vogt, L. H.; Katz, J. L.; Wiberley, S. E. *Inorg. Chem.* **1965**, *4*, 1157.

(18) Blatter, F.; Moreau, F.; Frei, H. *J. Phys. Chem.* **1994**, *98*, 13403.

(19) Landau, M. V.; Varkey, S. P.; Herskowitz, M.; Regev, O.; Pevzner, S.; Sen, T.; Luz, Z. *Microporous Mesoporous Mater.* **1999**, *33*, 149.

(20) Kruk, M.; Jaroniec, M.; Sakamoto, Y.; Terasaki, O.; Ryoo, R.; Ko, C. H. *J. Phys. Chem. B* **2000**, *104*, 292.

(21) Chen, C.-Y.; Li, H.-X.; Davis, M. E. *Microporous Mater.* **1993**, *2*, 17.

(22) Waysbort, D.; Navon, G. *Chem. Commun.* **1971**, 1410.

(23) Guenzburger, D.; Garnier, A.; Danon, J. *Inorg. Chim. Acta* **1977**, *21*, 119.

(24) Griffith, W. P. *J. Chem. Soc. A* **1966**, 899.

(25) Maltese, M. *J. Inorg. Nucl. Chem.* **1968**, *30*, 175.

(26) Waysbort, D.; Navon, G. *Inorg. Chem.* **1979**, *18*, 9.

(27) Stritar, J. A.; Taube, H. *Inorg. Chem.* **1969**, *8*, 2281.

(28) Allen, A. D.; Stevens, J. R. *Can. J. Chem.* **1973**, *51*, 92.

(29) Verdonck, E.; Vanquickenborne, L. G. *Inorg. Chem.* **1974**, *13*, 762.

(30) Fletcher, J. M.; Greenfield, B. F.; Hardy, C. J.; Scargill, D.; Woodhead, J. L. *J. Chem. Soc.* **1961**, 2000.

(31) Verdonck, J. J.; Schoonheydt, R. A.; Jacobs, P. A. *J. Phys. Chem.* **1981**, *85*, 2393.

(32) Broomhead, J. A.; Basolo, F.; Pearson, R. G. *Inorg. Chem.* **1964**, *3*, 826.

(33) Sugiura, C.; Kitamura, M.; Muramatsu, S. *J. Chem. Phys.* **1986**, *84*, 4824.

(34) Sham, T. K. *J. Am. Chem. Soc.* **1983**, *105*, 2269.

(35) Flood, M. T.; Ziolo, R. F.; Earley, J. E.; Gray, H. B. *Inorg. Chem.* **1973**, *12*, 2153.

(36) Addison, C. C.; Sutton, D. *Prog. Inorg. Chem.* **1967**, *8*, 195.

(37) Jørgensen, C. K. *Acta Chem. Scand.* **1956**, *10*, 887.

(38) Basila, M. R.; Kantner, T. R. *J. Phys. Chem.* **1967**, *71*, 467.

(39) Schmidt, K.; Hauswirth, W.; Müller, A. *J. Chem. Soc., Dalton Trans.* **1975**, 2199.

(40) Benesi, H. A.; Jones, A. C. *J. Phys. Chem.* **1959**, *63*, 179.

(41) Brodersen, K.; Becher, H. J. *Chem. Ber.* **1956**, *89*, 1487.

(42) Niwa, K.; Takahashi, H.; Higasi, K.; Kajiura, T. *Bull. Chem. Soc. Jpn.* **1971**, *44*, 3010.

(43) Sacconi, L. In *Transition Metal Chemistry*; Carlin, R. L., Ed.; Dekker: New York, 1968; Vol. 4, p 199.

(44) Thomas, J. M.; Sankar, G. *Acc. Chem. Res.* **2001**, *34*, 571.

(45) Blasse, G. *Struct. Bonding* **1991**, *76*, 153.

(46) Carriat, J. Y.; Che, M.; Kermarec, M.; Verdaguer, M.; Michalowicz, A. *J. Am. Chem. Soc.* **1998**, *120*, 2059.

(47) Zhao, X. S.; Lu, G. Q.; Whittaker, A. K.; Millar, G. J.; Zhu, H. Y. *J. Phys. Chem. B* **1997**, *101*, 6525.